Supporting Information

Evaluating Diabetic Ketoacidosis *via* MOF Sensor for Fluorescence Imaging of Phosphate and pH

Xue Wang,[†] Jin Li,[†] Wei Zhang,* Ping Li, Wen Zhang, Hui Wang, and Bo Tang*

College of Chemistry, Chemical Engineering and Materials Science, Collaborative Innovation Center of Functionalized Probes for Chemical Imaging in Universities of Shandong, Key Laboratory of Molecular and Nano Probes, Ministry of Education, Institute of Biomedical Sciences, Shandong Normal University, Jinan 250014, P. R. China.

[†]X. Wang and J. Li contributed equally.

E-mail: tangb@sdnu.edu.cn; zhangwei@sdnu.edu.cn

Diabetic ketoacidosis is one of the most common acute complications in diabetic patients. It is of great significance to develop a rapid and convenient method for the evaluation of diabetic complications-ketoacidosis. Herein, we prepared a novel composite metal-organic skeleton probe for simultaneous fluorescence detection and imaging of phosphate and pH in diabetic models. This work provides a new way to effectively evaluate the diabetic complication-ketoacidosis in the early clinical stage.

Table of Contents

Experimental

1. Materials and instrumentations

Materials. $ZrOCl_2 \cdot 8H_2O$, 2, 5-dihydroxy terephthalic acid, 4-formylbenzoic acid, pyrrole, reduced glutathione (GSH), ascorbic acid, Adenosine triphosphate (ATP) were purchased from Shanghai Maclin Biochemical Technology Co., LTD. L-cysteine (L-Cys), 3-(4, 5-dimethylthiazole-2 -)-2, 5-diphenyltetrazolium bromide (MTT) were purchased from Shanghai Sigma-Aldrich Reagent Co., LTD. N, N-dimethylformamide, propionic acid, dichloromethane, hydroquinone, hydrogen peroxide, ethylenediamine, K_3PO_4, Na_2SO_3, $NaSO_4$, $Na_2S_2O_3$, Na_2CO_3, $NaHCO_3$, NaCl, KBr, KI, $NaNO_3$, formaldehyde, glucose, fructose, and galactose were purchased from Sinopharm Chemical Reagent Co., Ltd. (Shanghai, China).

Synthesis of Al-BDC-NH_2. At room temperature, 272 mg (1.5 mmol) 2-amino terephthalic acid was dissolved in 60 mL DMF and heated to 110 ℃ in an oil bath, then 724 mg (3 mmol) $AlCl_3 \cdot 6H_2O$ was added in 7 equal parts at an interval of 10 min. The mixture was stirred at 110 ℃ for 3 h after the last part was added, and the stirring was stopped and kept at 110 ℃ for 16 h. After the reaction, the sediment was cooled to room temperature and centrifuged at 13,000 rpm for 10 min to collect. The yellow product was placed in a vacuum drying oven overnight.[1]

Synthesis of 5,10,15,20-Tetra(4-carboxyphenyl)porphyrin. The 5,10,15,20-Tetra(4-carboxyphenyl)porphyrin was prepared according to a reported method,[2] under the protection of N_2, added 400 mL redistilled propionic acid and 2.8

mL pyrrole into a 1000 mL three-necked round bottom flask, added 4-formylbenzoic acid (6 g, 0.04 mol), heated to 140 °C and reflux Stir for 1 h. After the reaction, it was reduced to room temperature and recrystallized at low temperature in dark place for 6 h to precipitate brown precipitation. Then suction filter the reaction solution and wash with dichloromethane until the crystal turns red brown and the washing solution is clear, and transfer the crystal to a vacuum drying oven to avoid light over night.

Synthesis of Al-MOF@PCN-224. $ZrOCl_2 \cdot 8H_2O$ (0.030 g), 5, 10, 15, 20-tetragarboxyphenyl) porphyrin (0.030 g) and benzoic acid (0.56 g) were dissolved in 20 mL DMF and dissolved by ultrasound for 5 min in a 100 mL flask. Then 30 mg Al-BDC-NH_2 was added to the mixture, and ultrasound was continued for 10 min to make it fully dissolved. After stirring at 90 ℃ for 5 h in oil bath, the product was cooled to room temperature and centrifuged at 14000 rpm for 20 min to collect the product. After repeated washing with DMF and anhydrous ethanol, the product was placed in a vacuum drying oven overnight.[3]

2. Instrumentations

Fluorescence Spectrometer (F-4700 HITACHT), ZHP-100 Constant temperature shaking incubator, UV-visible spectrophotometer (TU-1900), enzyme-labeled instrument (Synergy 2, Biotek, USA), DZF-6090 Vacuum drying oven, Zeta Potentiometer and DLS Dynamic light scatterometer (Malvern instruments Nano-ZS90), D8 ADVANCE X-ray powder diffractometer, Two-photon fluorescence microscope (Zeiss LSM 800 NLO), Electron microscope (HZTACHI HT7700),

Analytical Balances (AR224CM), Eppendorf low-temperature high-speed centrifuge (Centrifuge 5430R), FLS1000 Photoluminescence Spectrometer, Edinburgh Instruments Ltd..

3. Fluorescence lifetime test

The PL decay curves were measured by a fluorescence spectrophotometer (Edinburgh FSL1000) using a 60 W μs flash lamp (or xx nm pulse laser/LED) as an excitation light source.

4. Cell experiment

Cell culture: Liver cancer cells and liver cells were cultured in DMEM containing 1 % antibiotics and 10 % FBS and placed in a cell incubator containing 5 % CO_2 at 37 ℃.

5. Establishment of diabetic mouse model

Fifteen 5-week-old female C57BL/ 6J mice were divided into two groups: control group (n = 6) and diabetic group (n = 9). After one week of adaptive feeding, the fasting body weight of mice was measured after breaking feed for 12 h (continuous water). Mice in model group were intraperitoneally injected with 100 μL streptozotocin (STZ, 150 mg/kg, soluble in sodium citrate solution at pH 4.20) to establish the model, and control group mice were injected with the same dose of sodium citrate buffer as control. The diet was resumed after the injection. After 3 days, the fasting body weight of the mice was measured after breaking feed for 12 h, and the fasting blood glucose of the mice was measured with Roche blood glucose meter. All animal testing protocols are in accordance with the animal management regulations of the Ministry of Health of the People's Republic of China and have been

approved by the Animal Care Committee of Shandong Normal University.

6. Two-photon *in situ* imaging

Two-photon *in situ* imaging of pH and phosphate in liver and kidney organs of diabetic mice. The mice in both groups were anesthetized after intraperitoneal injection of 150 μL probe (200 μg/mL) for 1 hour. The epidermis of the mice was cut open to expose the liver and kidney organs, and two-photon in situ imaging of the liver and kidney organs was performed. The excitation wavelengths were 690 nm and 830 nm, respectively, and the fluorescence was respectively collected at 370-550 nm and 600-740 nm. The experiment was carried out for 5 times in each group.

Results and Discussion

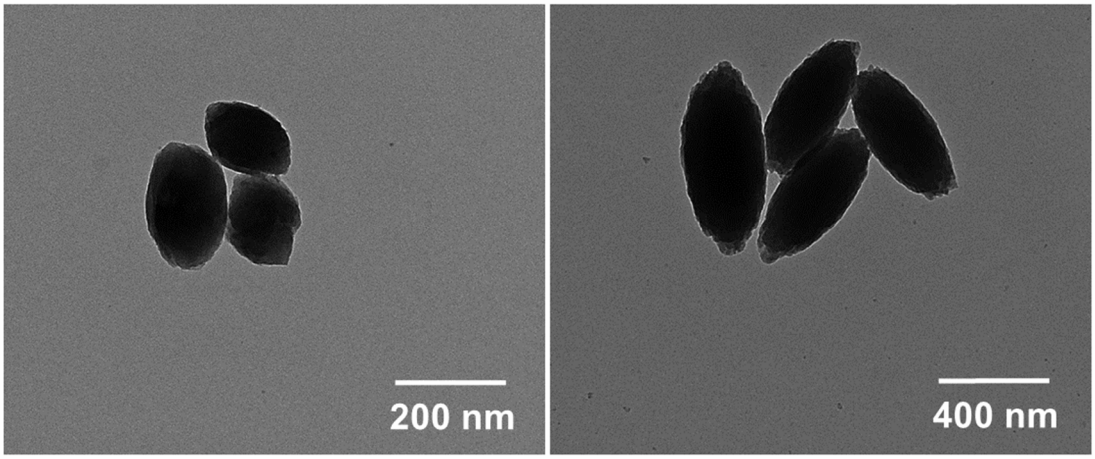

Figure S1. TEM of the Al-MOF (left) and Al-MOF@PCN-224 (right).

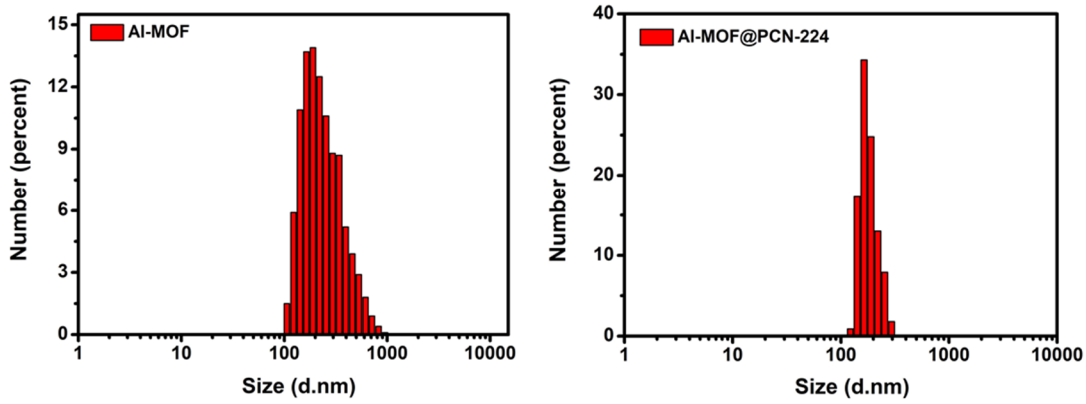

Figure S2. Hydrate particle size of the Al-MOF and Al-MOF@PCN-224.

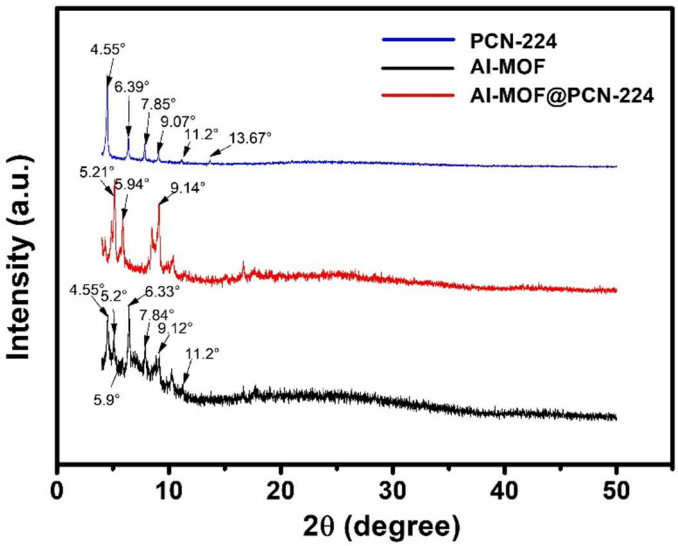

Figure S3. PXRD of the PCN-224, Al-MOF and Al-MOF@PCN-224. [4,5]

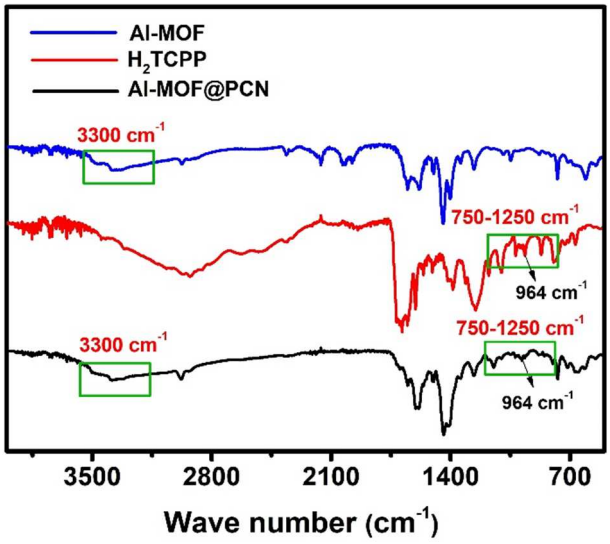

Figure S4. Infrared spectrum of the Al-MOF, porphyrin and Al-MOF@PCN-224.

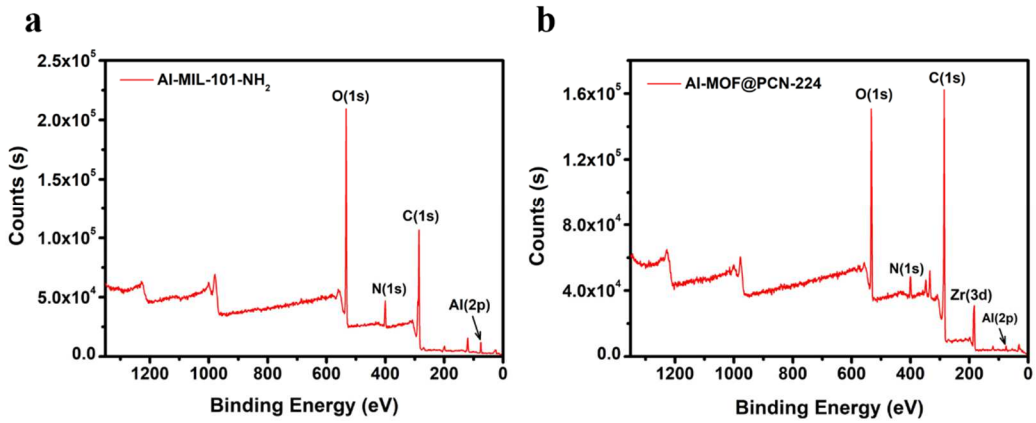

Figure S5. X-ray photoelectron spectroscopy (XPS) of the material.

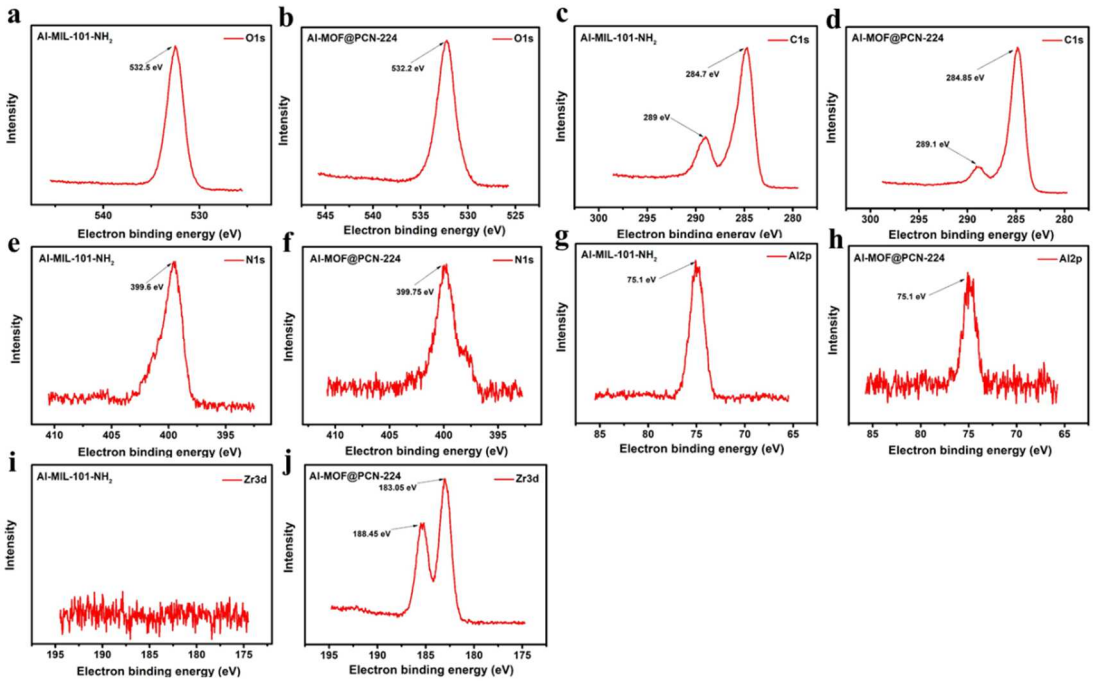

Figure S6. XPS spectra of different elements in different samples. (a), (c), (e), (g), (i) XPS spectra of Al-MIL-101-NH_2; (b), (d), (f), (h), (j) XPS spectra of Al-MOF@PCN-224.[7-11]

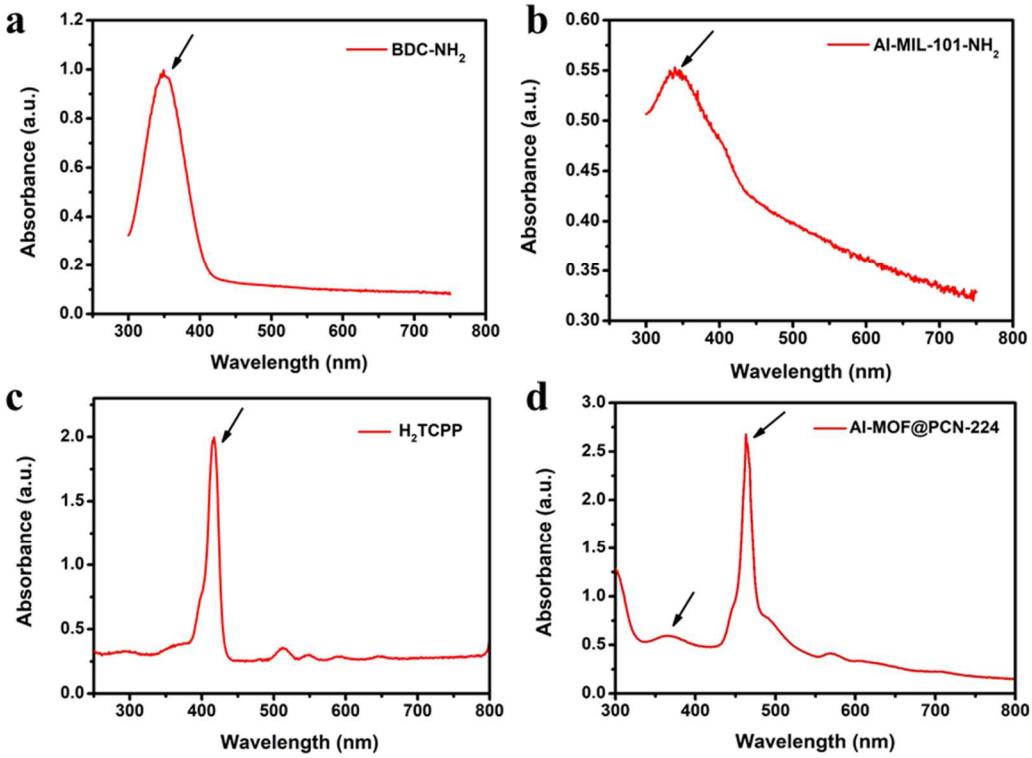

Figure S7. Ultraviolet absorption spectrum of (a) 2-amino-terephthalic acid, (b) Al-MIL-101-NH_2, (c) porphyrin and (d) Al-MOF@PCN-224.

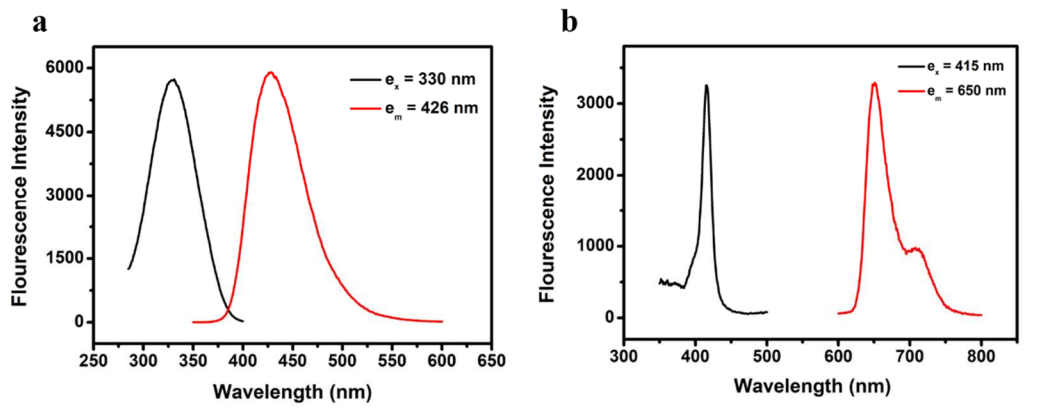

Figure S8. Fluorescence excitation and emission spectra of the Al-MOF@PCN-224。

The two maximum excitation peaks and emission peaks of Al-MOF@PCN-224.

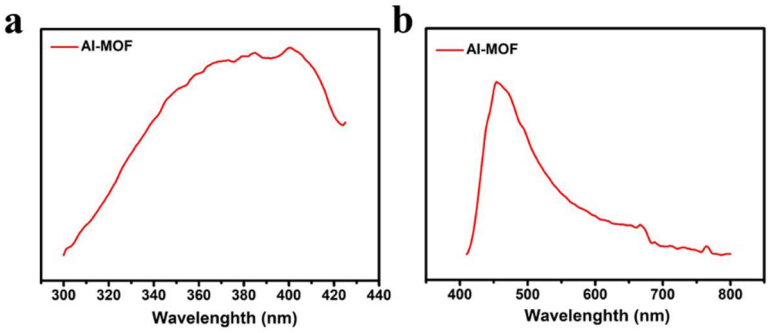

Figure S9. Absorption spectrum (a) and fluorescence spectrum (b) of Al-MOF solid powder, fluorescence spectrum experimental conditions: λ_{ex}=380 nm.

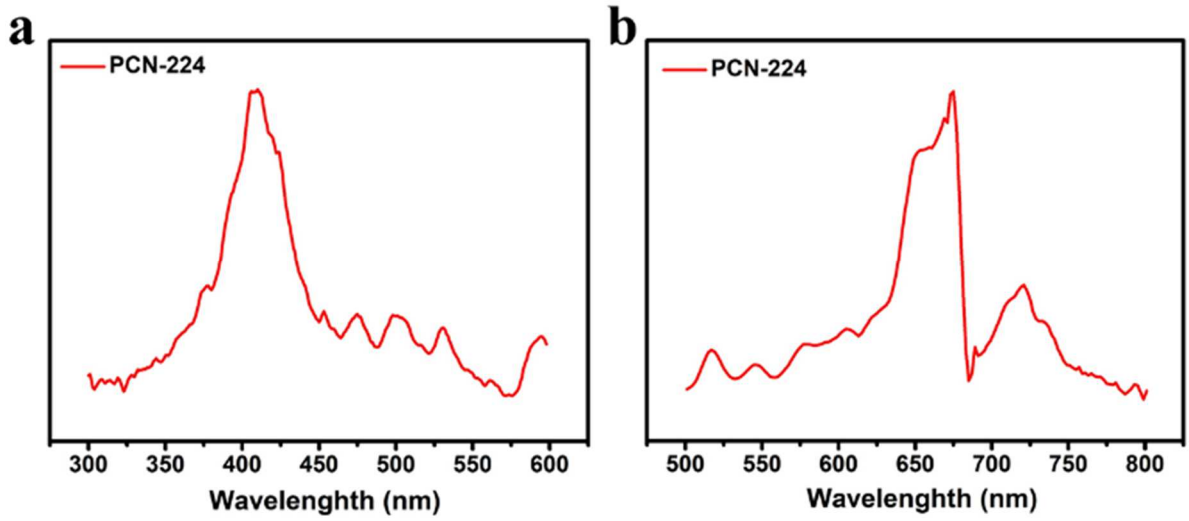

Figure S10. Absorption spectrum (a) and fluorescence spectrum (b) of PCN-224 solid powder, fluorescence spectrum experimental conditions: λ_{ex}=415 nm.

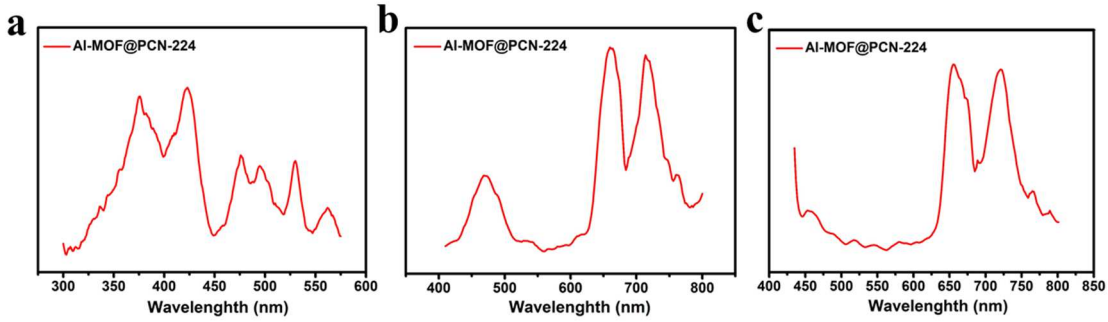

Figure S11. Absorption spectrum (a) and fluorescence spectrum (b) and (c) of Al-MOF@PCN-224 solid powder, fluorescence spectrum experimental conditions: (b): λ_{ex}=380 nm,(c) λ_{ex}=415 nm.

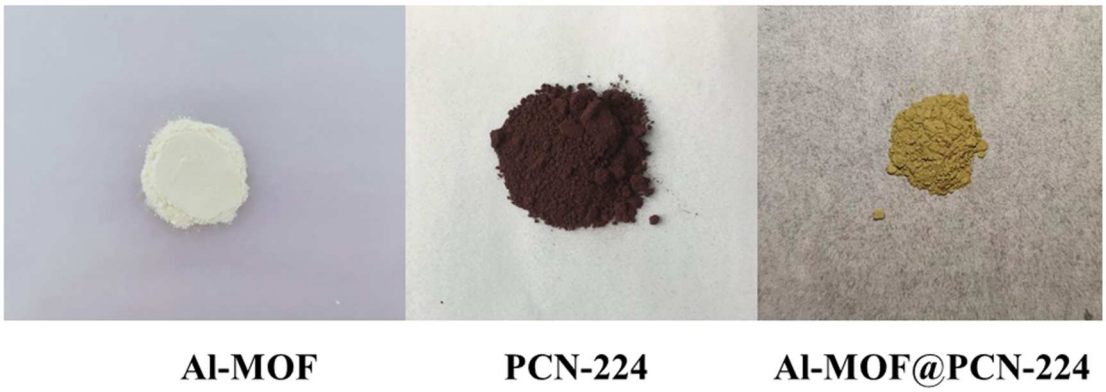

Figure S12. Images of Al-MOF,PCN-224 and Al-MOF@PCN-224.

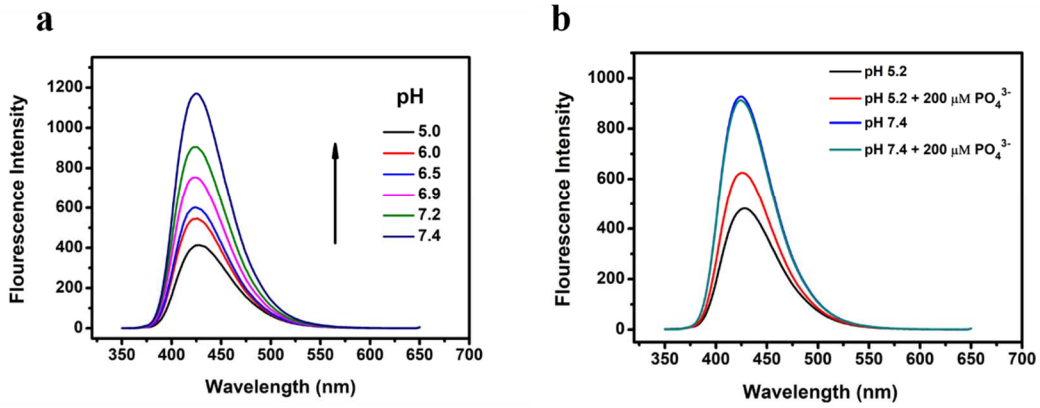

Figure S13. (a) Fluorescence spectra of the probe in HEPES buffer solutions of different pH (20 mM). (b) Fluorescence spectra of the probe in HEPES buffer solutions of pH 5.2 and 7.4, respectively, with 200 μM phosphoric acid. Experimental conditions: λ_{ex} = 330 nm.

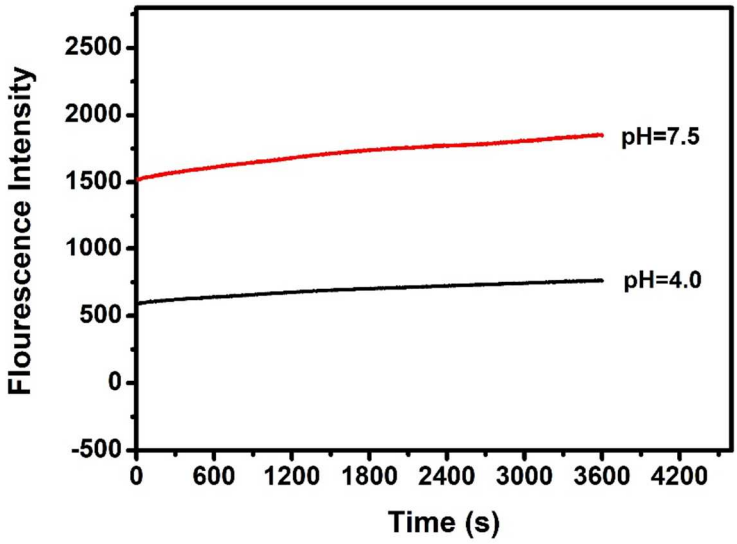

Figure S14. Dynamics experiments at Al-MOF@PCN-224. Experimental conditions: λ_{ex} = 330 nm.

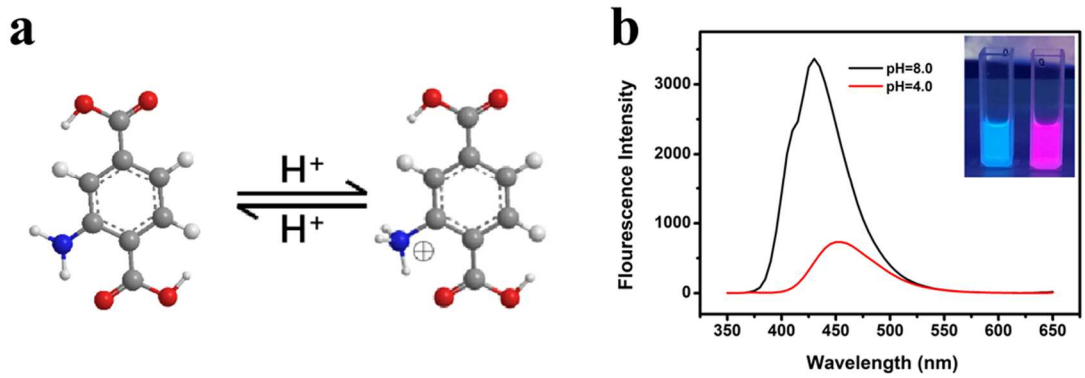

Figure S15. Schematic diagram of the probe sensing mechanism. (a) Schematic diagram of sensor based on protonation of nitrogen atom in amino group. (b) Fluorescence spectra of the probe at pH 4.0 and 8.0. The pictures of the probe under UV lamp at pH 4.0 and 8.0 are illustrated.

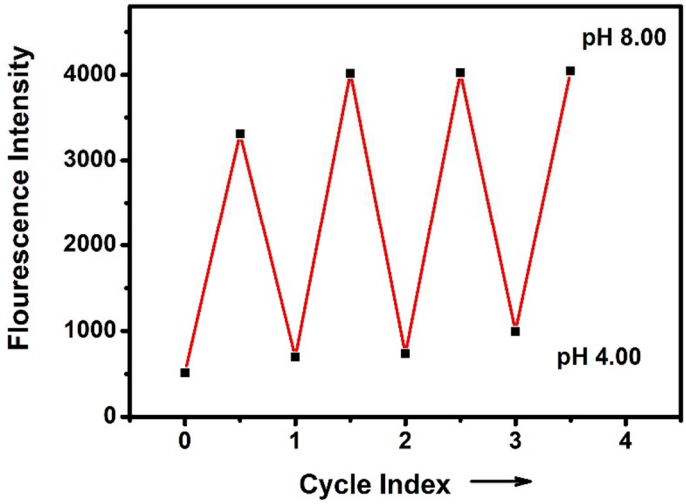

Figure S16. The reversibility of Al-MOF@PCN-224 in aqueous solution with pH between 4.00 and 8.00. Experimental conditions: λ_{ex} =330 nm.

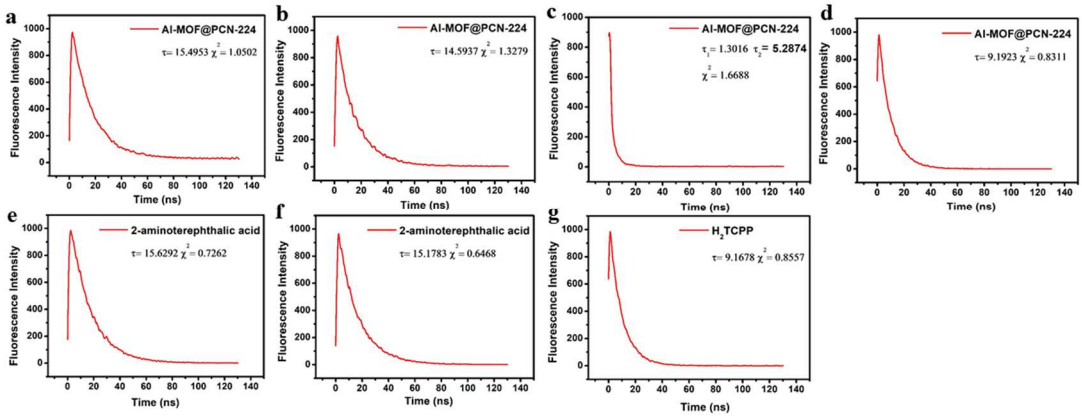

Figure S17. The PL lifetimes of Al-MOF@PCN-2214 with H_2TCPP and terephthalic acid. Experimental conditions: a) Laser: 340 nm, pH = 8.0, 5 mM phosphatecitric acid buffer , $C_{Al\text{-}MOF@PCN}$ = 25 μg/mL; b) Laser: 340 nm, pH = 4.0, 5 mM phosphatecitric acid buffer, $C_{Al\text{-}MOF@PCN}$ = 25 μg/mL; c) Laser: 405 nm, pH = 7.4, 20 mM HEPES buffer, $C_{Al\text{-}MOF@PCN}$ = 25 μg/mL; d) Laser: 405 nm, pH = 7.4, $C_{Al\text{-}MOF@PCN}$ = 25 μg/mL, PO_4^{3-} = 200 μM, 20 mM HEPES buffer; e) Laser: 340 nm, pH = 8.0, 5 mM phosphatecitric acid buffer; f) Laser: 340 nm, pH = 4.0, 5 mM phosphatecitric acid buffer; g) Laser: 405 nm, pH = 7.4, 20 mM HEPES buffer.

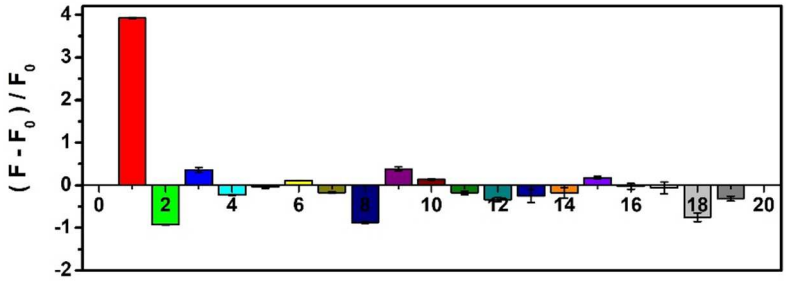

Figure S18. Probe response to phosphate and other interfering substances: 1. PO_4^{3-} (200 μM), 2. SO_4^{2-} (1 mM), 3. SO_3^{2-} (1 mM), 4. NO_3^- (1 mM), 5. CO_3^{2-} (1 mM), 6. HCO_3^- (200 μM), 7. Br^- (1 mM), 8. Cl^- (1 mM), 9. ATP (1 mM), 10. GSH (1 mM), 11. D-cys (200 μM),12. ClO^- (200 μM), 13. H_2O_2 (200 μM), 14. ·OH (100 μM), 15. $_1O^2$(100 μM), 16. $O_2\cdot^-$ (100 μM), 17. NO (100 μM), 18. pH = 6.0, 19. pH = 6.8.

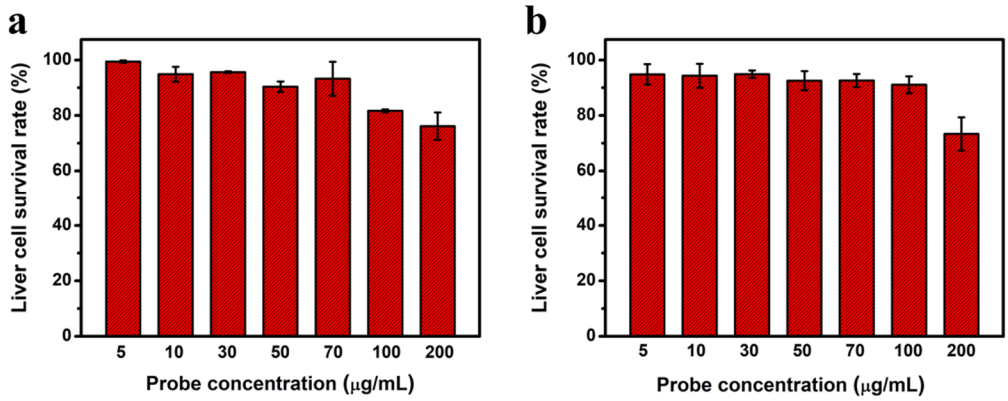

Figure S19. The cell survival rate varied with Al-MOF@PCN-224 concentration. (a) liver cancer cells, (b) liver cells, indicating that the probe has good biocompatibility.

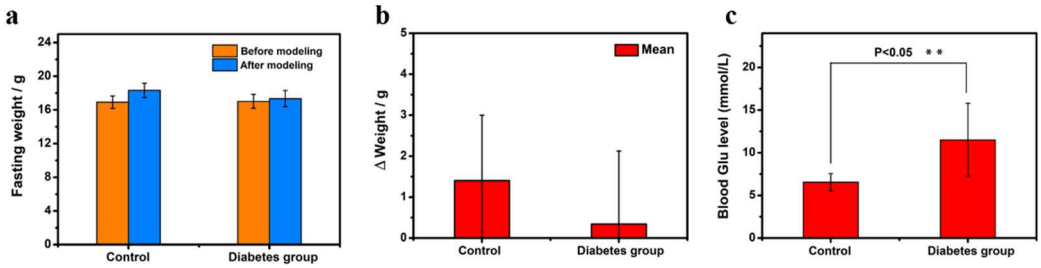

Figure S20. Changes of various indexes of mice before and after modeling. (a) Fasting weight. (b) Weight changes. (c) Blood glucose levels.

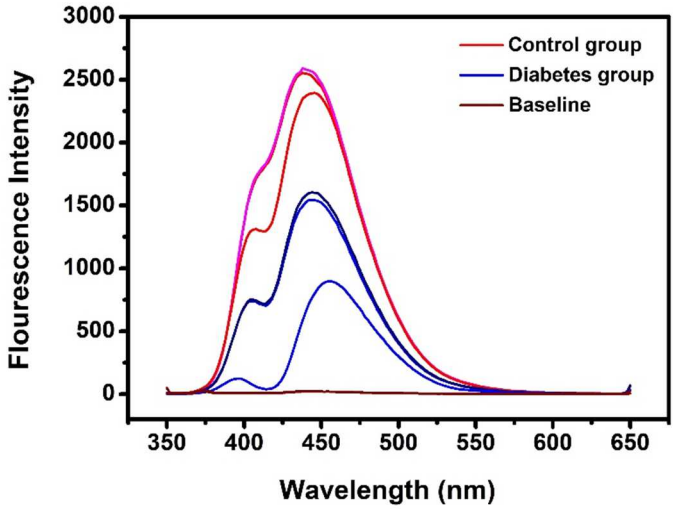

Figure S21. Comparison of pH (λ_{ex} = 330 nm) in serum of mice in model group and normal group.

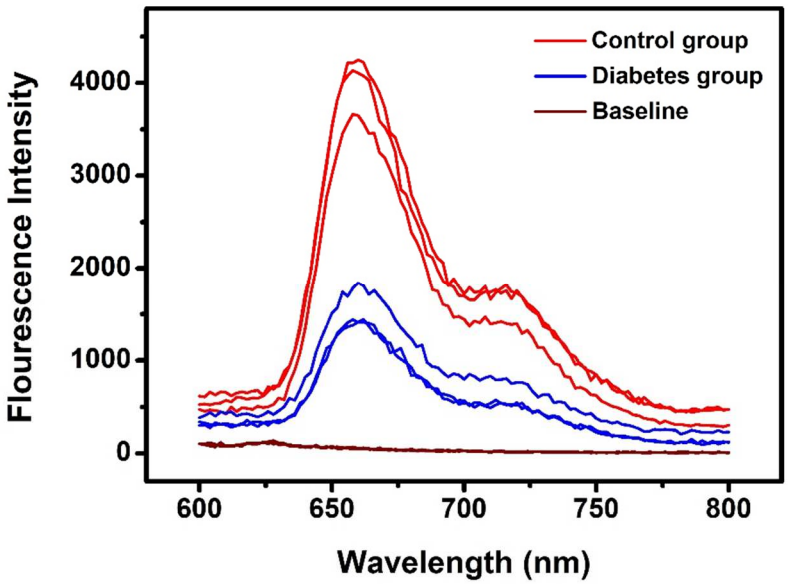

Figure S22. Comparison of phosphoric acid levels (λ_{ex} = 415 nm) in serum of mice in model group and normal group.

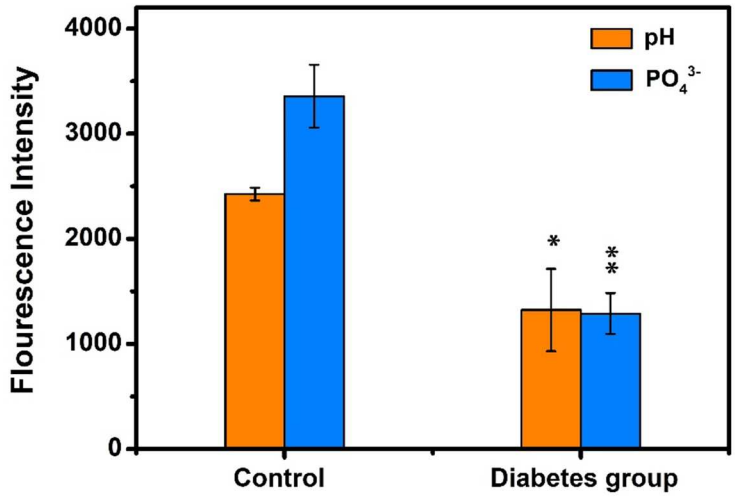

Figure S23. Intensity output diagram of serum test results.

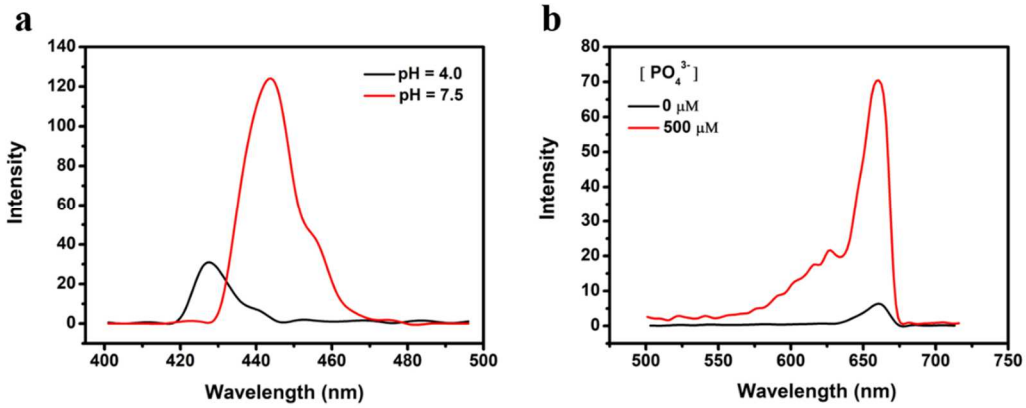

Figure S24. Two-photon properties of the probe, the results are consistent with the reported two-photon properties of ligand molecules. Experimental conditions: C_{MOFs} = 300 μg/mL, 20 mM HEPES, pH=7.4, (a) λ_{ex} = 690 nm, (b) λ_{ex} = 830 nm.

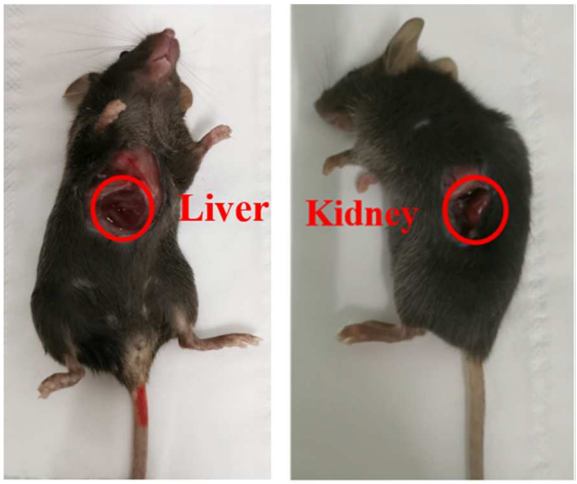

Figure S25. Protocol for *in situ* imaging of mice liver and kidney.

References

1. X. Y. Xu, B. Yan, *Dalton Trans.*, 2016, **45** ,7078-108.
2. W. Zhang, J. Xu, P. Li, X. Gao , W. Zhang,H. Wang, B. Tang, *Chem. Sci.*, 2018, **9**, 7483-7487.
3. J. Park, Q. Jiang, D. Feng, L. Mao, H-C. Zhou, *J. Am. Chem. Soc.*, 2016, **138**, 3518-3525.
4. S.Ahmadipouya, F. Ahmadijokani, H. Molavi, M. Rezakazemi, M. Arjmand, *Chem. Eng. Res. Des.*, 2021, **176**, 49-59.
5. R.Shi, D. Lv, Y. Chen, H. Wu, B. Liu, Q. Xia, Z. Li, *Sep. Purif. Technol.*, 2018, **207**, 262-268.
6. M. Smith, L. Scudiero, J. Espinal, J. McEwen, M. Garcia-Perez, *Carbon*, 2016, **110**, 155-171.
7. J. R. Zhang , Y. Ma , S. Y. Wang , J. Ding , B. Gao , E. Kan, W. Hua , *Phys. Chem. Chem. Phys.*, 2019, **21**, 22819-22830.
8. J.-K. Sun, Q. Xu , *Chem. Commun.*, 2014, **50**, 13502-13505.
9. A. Lyapin, L.P.H. Jeurgens, P.C.J. Graat, E.J Mittemeijer, *J. Appl. Phys.*, 2004, **96**, 7126-7135
10. W. Zhang, X. Liu, P. Li, W. Zhang, H. Wang, B. Tang, *Anal. Chem.*,2020, **92**, 3716-3721.
11. W. Zhang, J. Ren, J. Lu, P. Li, W. Zhang, H. Wang, B. Tang, *Anal. Chem.* , 2021, **93**, 10907–10915.